ELECTROMAGNETIC FIELD IN ANECHOIC AND EMC CHAMBERS – PART 1 - MODELLING

Miloš MAZÁNEK, Martin KLEPAL, Pavel PECHAČ
Dept. of Electromagnetic Field
Czech Technical University
Technická 2, K317, 166 27 Prague
Czech Republic

Abstract

Anechoic and EMC chamber at the CTU in Prague was designed and used for a variety of antenna measurements and EMI testing. Due to different measurement methods (near field, far field, compact range, and EMI measurement) applied in the laboratory, different simulations were performed during the design process.

Keywords

anechoic chamber, EMI measurement, electromagnetic field modelling

1. Introduction

During the anechoic (EMC) chamber design process it is necessary to discuss the power budget with respect of "industrial outer noise" and parasitic reflection of inner transmitter. Quiet zone calculation based on the Ray-tracing method is described. The criteria has to follow the final measurement methods which should be implemented in the laboratory (far field, near field, CATR, holographic principles, as well as standard EMI testing methods). The modelling described in this paper and measurement results in its Part 2 should contribute to the answers in these fields:

- shape and dimensions of the chamber
- transmitting (illuminating) antenna
- absorbents and shielding

Each of these items above contains a lot of other questions. Answers will differ depending on the measurement method and type of the device under the test. Usually there is no a general rule but some of the results of modelling can contribute to the better understanding of the problem in complexity (e.g. what chamber dimensions and what antenna radiation patters fit best to the antenna testing).

2. Modelling

2.1 Analysis

Intensity of electromagnetic filed E_{max} in a distance r is expressed in term of transmitted power P_t – equations (1),(2),(3).

$$S = \frac{1}{2} \cdot \frac{E_{\max}^{\ 2}}{120\pi} \tag{1}$$

$$P = S 4\pi r^2 = \frac{1}{2} \cdot \frac{E_{\max}^{\ 2}}{120\pi} 4\pi r^2 = \frac{E_{\max}^{\ 2}}{60} r^2 \tag{2}$$

$$E_{\max} = \frac{\sqrt{P_t 60}}{r} \tag{3}$$

Gain for horizontal and vertical component can be used from modelling as well as from measurement (4)

$$\begin{aligned} \boldsymbol{G}_{tH} &= G_{tH} \mathrm{e}^{\mathrm{j}\phi_{tH}} \boldsymbol{e}_{OH} \qquad & \boldsymbol{G}_{tV} &= G_{tV} \mathrm{e}^{\mathrm{j}\phi_{tV}} \boldsymbol{e}_{OV} \\ \boldsymbol{G}_{rH} &= G_{rH} \mathrm{e}^{\mathrm{j}\phi_{rH}} \boldsymbol{e}_{OH} & \boldsymbol{G}_{rV} &= G_{rV} \mathrm{e}^{\mathrm{j}\phi_{rV}} \boldsymbol{e}_{OV} \end{aligned} \tag{4}$$

From (3) for individual E field components valid

$$\boldsymbol{E}_H = E_H \mathrm{e}^{\mathrm{j}\varphi_H} \boldsymbol{e}_{OH} \qquad \boldsymbol{E}_V = E_V \mathrm{e}^{\mathrm{j}\varphi_V} \boldsymbol{e}_{OV} \tag{5}$$

$$|\boldsymbol{E}_H|^2 + |\boldsymbol{E}_V|^2 = |\boldsymbol{E}|^2 = \frac{P_t 60}{r^2} \tag{6}$$

Intensity of electrical field is calculated from horizontal and vertical components for both – direct and reflected rays (Fig. 1, Fig. 2, Tab. 1, Tab 2, Fig. 3, and finally Fig. 4) – V1,V2,H1,H2 using distances r_1, r_2 . (example equation (7))

$$\boldsymbol{E}_{rH} = E_t \sqrt{G_{rH}\, G_{tH}}\, \boldsymbol{R}_H \mathrm{e}^{-\mathrm{j}kr} \tag{7}$$

Total receiving power (10) is calculated from power density (8), antenna effective area (9) – using efficiency factor between antenna gain and its directivity

$$\boldsymbol{S} = \frac{P_t \boldsymbol{G}_t}{4\pi r^2} \mathrm{e}^{-\mathrm{j}kr} \tag{8}$$

$$A_{ef} = D_p \frac{\lambda^2}{4\pi} \tag{9}$$

$$P_r = \left| S_1 A_{ef1} + S_2 A_{ef2} \right| \eta_r \tag{10}$$

and finally

$$P_r = P_t \left(\frac{\lambda}{4\pi} \right)^2 \left| \frac{\sqrt{G_{t1} G_{r1}}}{r_1} e^{-jkr_1} + \frac{\sqrt{G_{t2} G_{r2}}}{r_2} e^{-jkr_2} \right|^2 \tag{11}$$

Total receiving power is equal to the sum of horizontal and vertical component

$$P_r = P_{rh} + P_{rv} \tag{12}$$

and based on electrical field components

$$P_r = \left(\frac{\lambda}{4\pi} \right)^2 \frac{1}{60} \left(\left| E_{H1} + E_{H2} \right|^2 + \left| E_{V1} + E_{V2} \right|^2 \right) \tag{13}$$

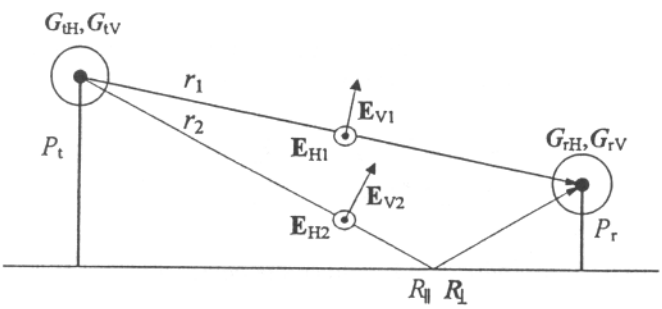

Fig. 1 Model of direct and reflected rays (t – transmitter, r - receiver, H – horizontal, V - vertical)

2.2 Anechoic chamber model

Eleven rays were taken into account during an anechoic chamber simulation (Fig. 4). The electrical field distribution in projection plane (Fig. 2) was calculated with respect of the proper sampling, transmitting (illuminating) and receiving antenna data (radiation pattern, gain), absorbent reflectivity, Tab. 1, Tab. 2, Fig. 3.

3. Results

Results of modelling are in Fig. 7 to 12.

Tab. 3 Antennas and chamber setup for modelling of electromagnetic field

Fig No.	Chamber	Radiator	Receiving antenna	Receiver polarisation
7	Anechoic	Isotropic	Isotropic	
8	Anechoic	Isotropic	Bi – log	
9	Semianech.	Isotropic	Isotropic	Vertical
10	Semianech.	Isotropic	Isotropic	Horizontal
11	Semianech.	Isotropic	Bi – log	Vertical
12	Semianech.	Isotropic	Bi – log	Horizontal

4. Conclusion

Results of modelling of the chamber specially for EMI testing in anechoic / semianechoic arrangement shows:

- Semianechoic arrangement cause high oscillations in the "measurement zone" and does not bring the "worst case measurement results" specially at the frequencies bellow 100 MHz.
- Horizontal and vertical polarisation of the testing antenna brings complementary results.
- Higher directivity antenna (e.g. bi-log) gives better results (lower oscillation in measurement zone) compare to less directive one.
- Open Area Test Site (semianechoic) and anechoic measurement can bring the theoretical 3-dB difference - then the EMI measurement in an anechoic arrangement seems to be more reliable.

Anechoic chamber of CTU was designed, modelled, build and tested. Method of testing description and results will be presented in a Part 2.

- electromagnetic noise background
- wall reflections
- uniformity of electromagnetic field
- path loss test of the anechoic room
- total wall shielding effectiveness.

References

[1] MAZÁNEK, M.: Anechoic and EMC chambers – Invited paper, Radioelectronika 98, Technical University Brno, 1998, pp. 1-12.

[2] MAZÁNEK, M. - PECHAČ, P.: Anechoic Chambers Testing, 43. IWK, Ilmenau, October 1998, pp. 307-310.

[3] MAZÁNEK, M. - KLEPAL, M. - PECHAČ, P. - POLÍVKA, M. - BÁRTÍK, H.: Anechoic and EMC Chambers – Modelling, Design, Testing. Millenium Conference on Antennas and Propagation AP2000, Vol. 2. April 2000 pp. 156.

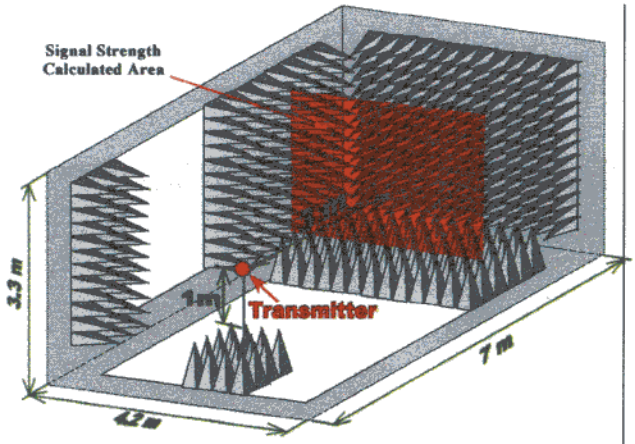

[4]

Fig. 2 Anechoic and EMC chamber modelling

Tab. 1 Absorbent and wall reflection parameters used for simulation. Reflection [dB] for normal incidence

f [GHz]	0.5	1	2	4	8	>12
R [dB]	-30	-35	-42	-50	-52	-53

Tab. 2 Reflection coefficient as a function of angle of incidence (0 degree ~ normal incidence)

Absorber Height / λ \ Incidence Angle γ	45°	50°	55°	60°	65°	70°	75°	80°
4.0	1.00	0.95	0.86	0.75	0.70	0.60	0.51	0.43
2.0	0.90	0.82	0.74	0.66	0.58	0.49	0.42	0.34
1.0	0.72	0.65	0.58	0.50	0.44	0.37	0.31	0.25
0.5	0.48	0.43	0.37	0.31	0.25	0.20		

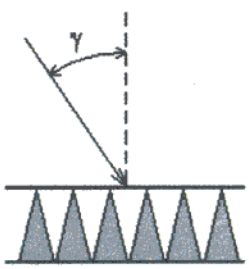

Fig. 3 Incidence angle geometry

Acknowledgement

This work has been conducted at the Department of Electromagnetic Field of Czech Technical University in Prague and supported by the Department, the project Antenna Laboratory VS 97035 of the Czech Ministry of Education and by the programme: Research in the Area of Information Technologies and Communications J04/98: 212300014

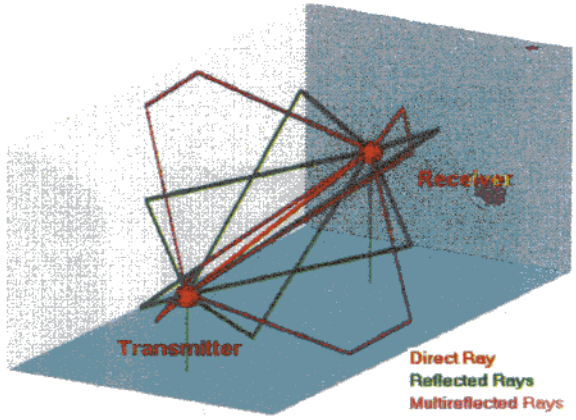

Fig. 4 Dominant Rays in Anechoic and EMC Chamber

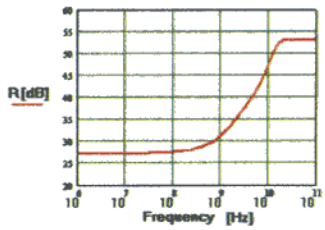

Fig. 5 Reflection for normal incidrence as a function of frequency

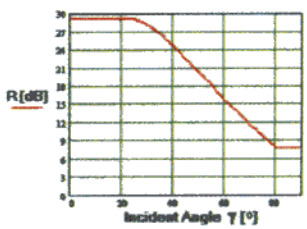

Fig. 6 Reflection coeficient as a function of incident angle at frequency 1 GHz

About authors...

Miloš MAZÁNEK was born in Tanvald 1950. He received his MSc. from the Faculty of Electrical Engineering of the Czech Technical University in 1974. He joined the Department of Electromagnetic Field, where he is now a head of the department. He has developed his research interests in microwave radiometry, antennas, propagation of electromagnetic waves, and electromagnetic compatibility. He is a member of IEEE, head of the Radioengineering Society, head of National Committee URSI F group and Radioengineering journal executive editor.

Martin KLEPAL – see page 36.

Pavel PECHAČ – see page 36.

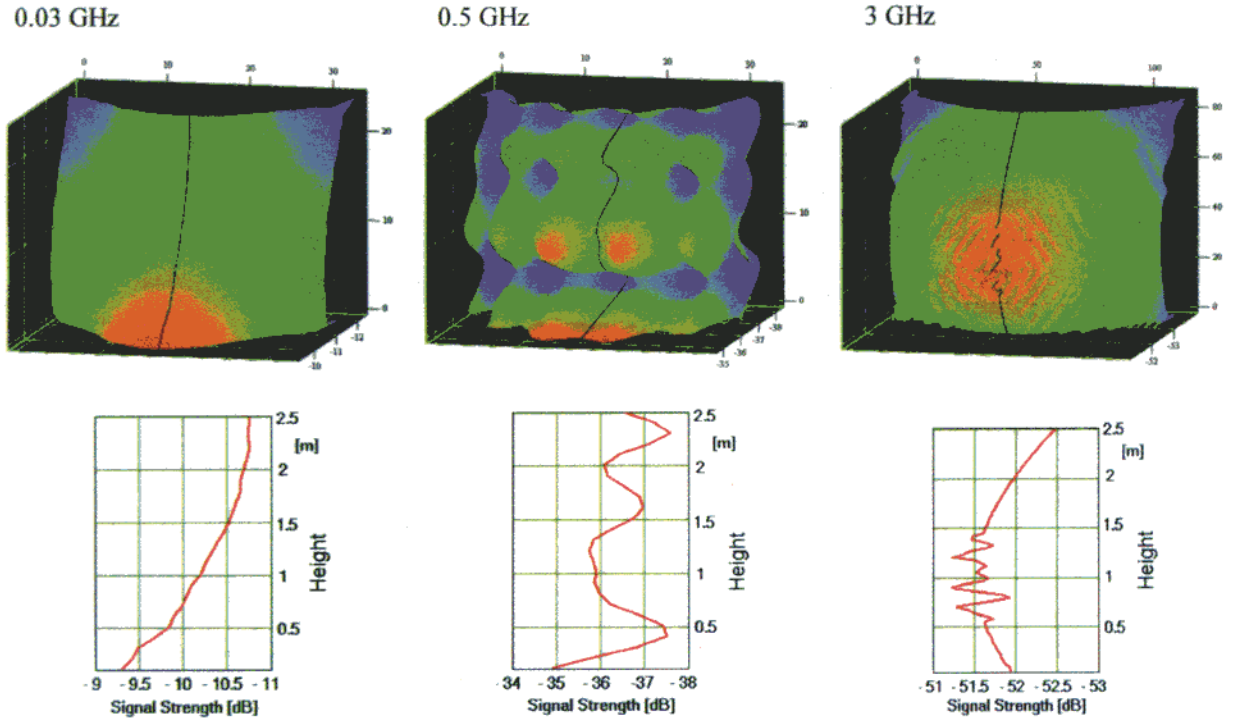

Fig. 7 Electromagnetic field modelling depending on frequency (geometry see Fig. 2, data see Tab. 3)

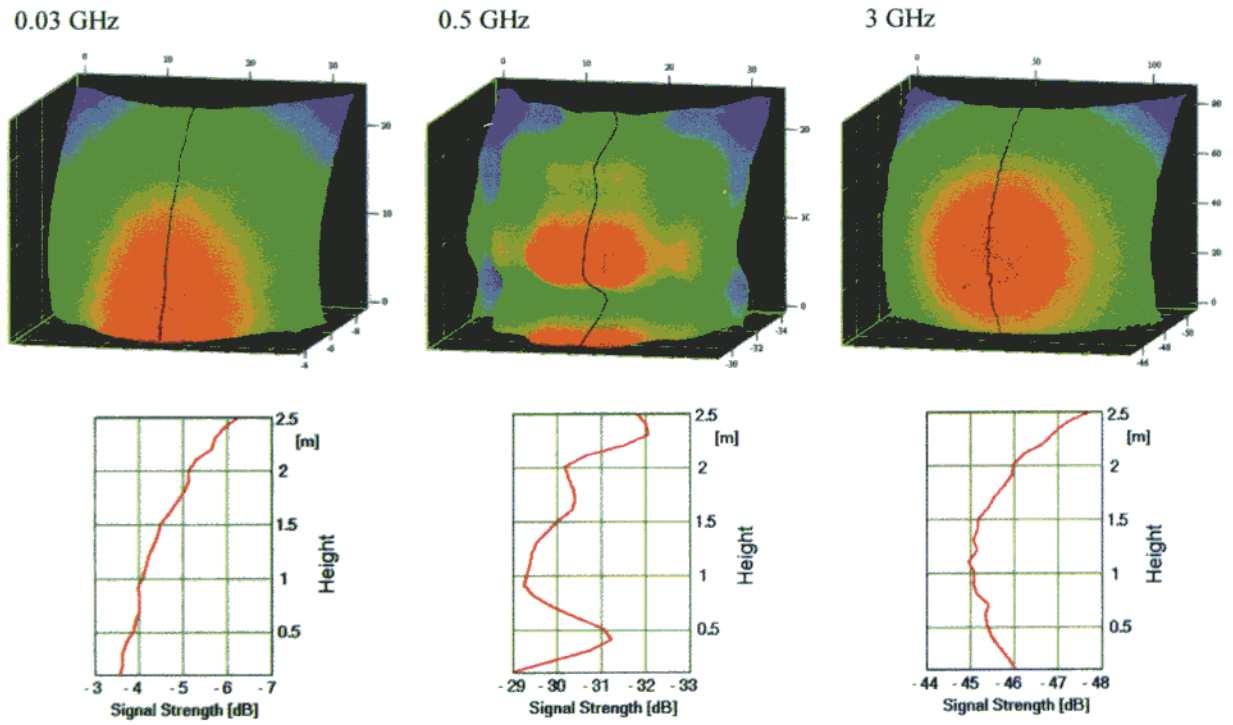

Fig. 8 Electromagnetic field modelling depending on frequency (geometry see Fig. 2, data see Tab. 3)

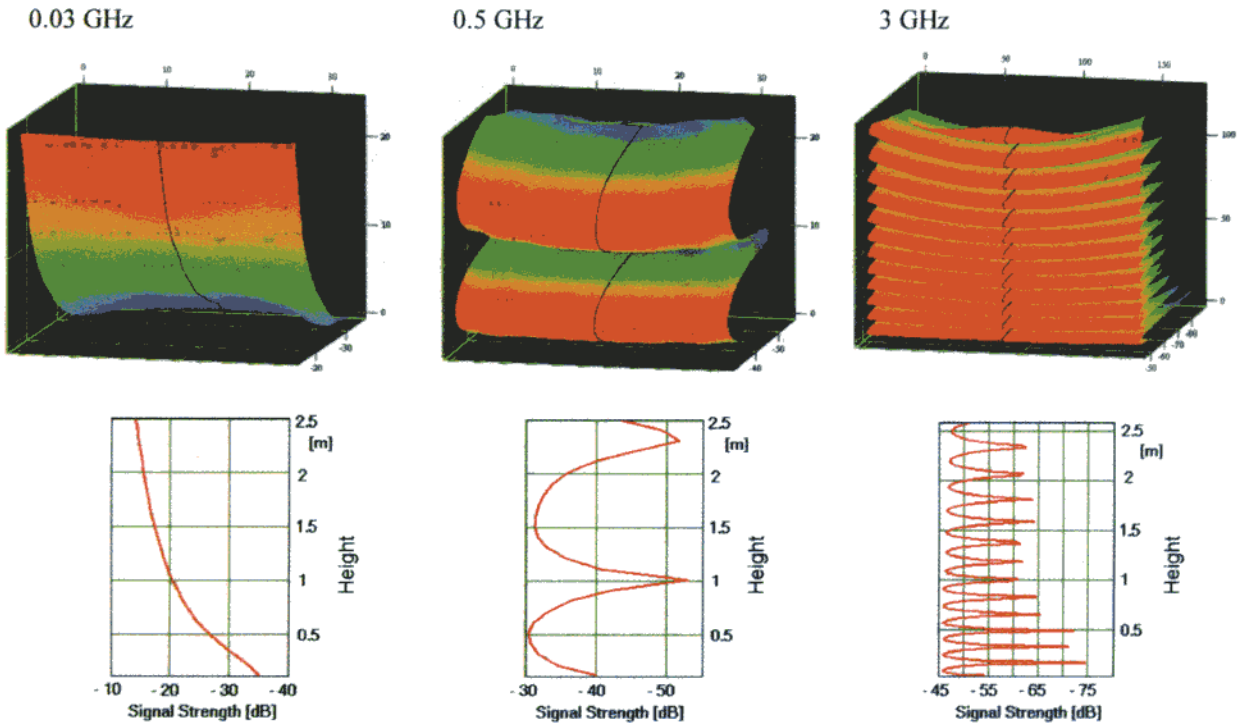

Fig. 9 Electromagnetic field modelling depending on frequency (geometry see Fig. 2, data see Tab. 3)

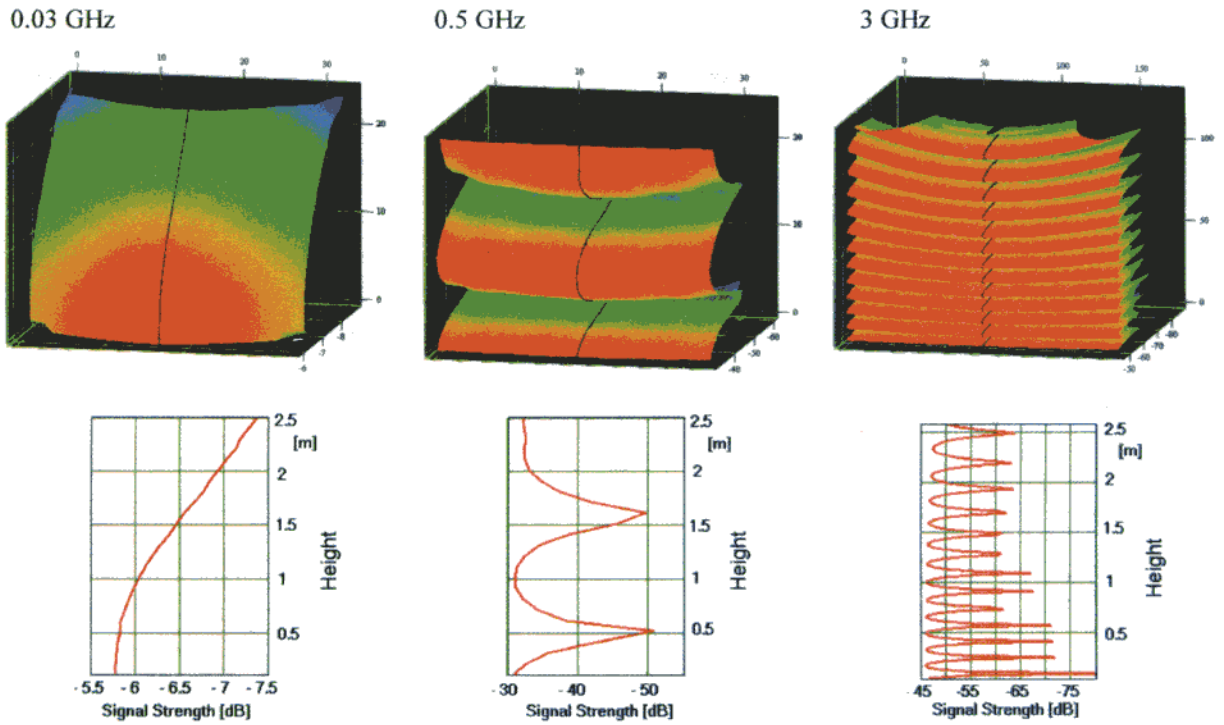

Fig. 10 Electromagnetic field modelling depending on frequency (geometry see Fig. 2, data see Tab. 3)

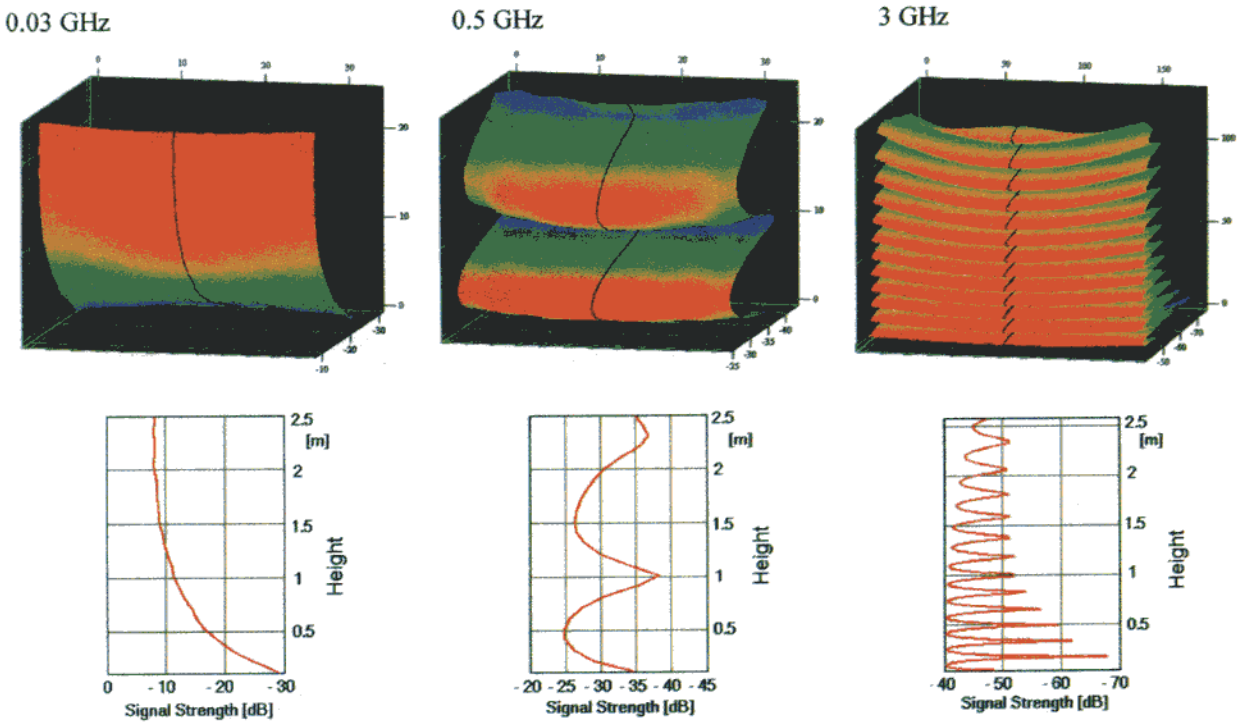

Fig. 11 Electromagnetic field modelling depending on frequency (geometry see Fig. 2, data see Tab. 3)

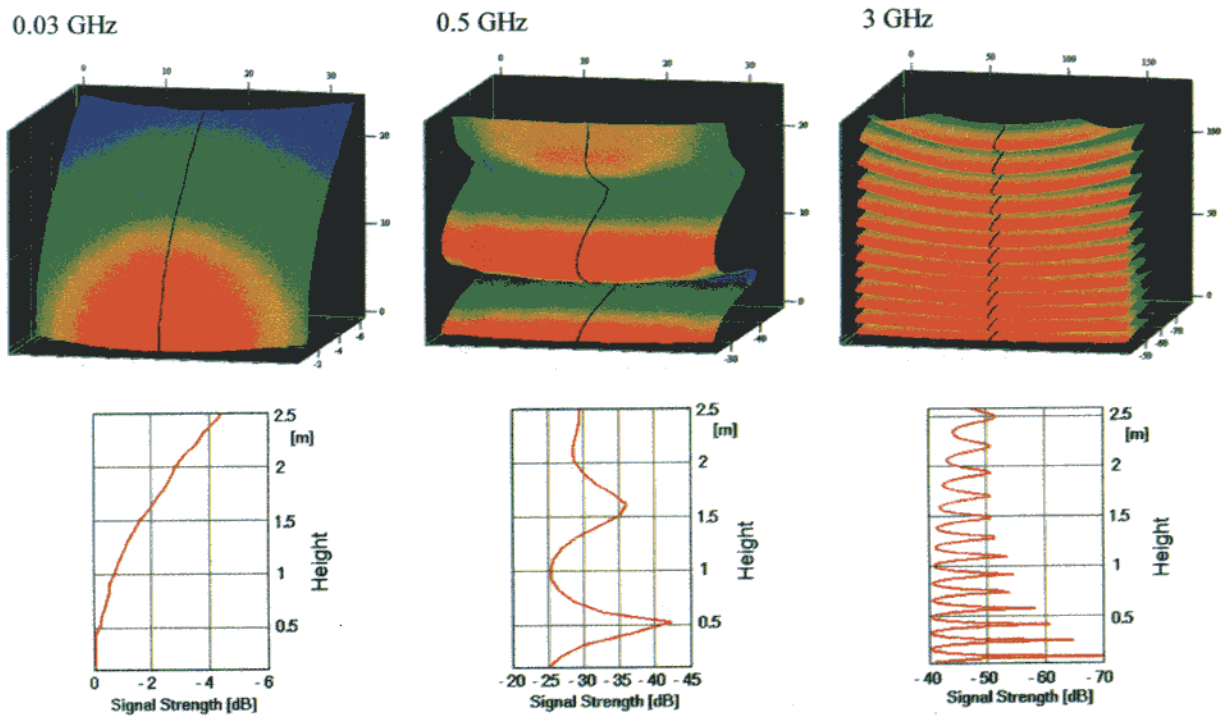

Fig. 12 Electromagnetic field modelling depending on frequency (geometry see Fig. 2, data see Tab. 3)